Journal of Petroleum
Science and Technology

An Injection Rate Optimization in a Water Flooding Case Study with an Adaptive Simulated Annealing Techniques

Vahid Azamipour and Mehdi Assareh*

Thermodynamics Research Laboratory, School of Chemical Engineering, Iran University of Science and Technology, Tehran, Iran

ABSTRACT

This paper introduces an effective production optimization and a water injection allocation method for oil reservoirs with water injection. In this method, a two-stage adaptive simulated annealing (ASA) is used. A coarse-grid model is made based on average horizon permeability at the beginning iterations of the optimization to search quickly. In the second stage, the fine-grid model is used to provide the accuracy of the final solution. A constrained optimization problem to maximize an objective function based on net present value is implemented. Allocation factors from the streamline simulation are used to help for the appropriate estimation of initial water injection rates. The proposed optimization scheme is used for a field sector simulation model. The results show that the optimized rates confirm the increment of total oil production. Optimized oil production and total water injection rates lead to an increase in the total oil production from 385.983 (initial guess) to 440.656 Msm^3. This means a recovery factor increment by 14.16%, while the initial rates were much higher than the optimized rates. Moreover, the recovery factor of optimized production schedule with an optimized total injection rate is 2.20% higher than the initial production schedule with an optimized total water injection rate. The allocation of the water injection rates and the revision of allocation rates result in 446.383 and 450.164 Msm^3. The revision of the water rates allocation provides a reduction of water cut during production.

Keywords: Life-Cycle Optimization, Adaptive Simulated Annealing, Water flooding, Streamline Simulation.

INTRODUCTION

In the context of oilfield development, the dynamic reservoir modeling and the production optimization have been attractive research areas. The complexity of geological models, facilities and the operational constraints complicate the formulation and solution of production optimization problems. Especially in large fields, because of the costs and complexities of the full simulation of a reservoir model, finding the optimized production strategies becomes very time-consuming, and it is practically impossible to derive all possible solutions. In fact, for the optimization of such problems, the efficiency and viability of the method are important subjects. The determination of a production scenario is one of the significant tasks in the reservoir management

***Corresponding author**
Mehdi Assareh
Email: assarehm@iust.ac.ir
Tel: +98 21 7724 3025
Fax: +98 21 7724 0495

Article history
Received: April 17, 2016
Received in revised form: December 28, 2016
Accepted: January 31, 2017
Available online: November 15, 2017

because it affects the total oil production and project benefit. Many studies have been carried out to improve the reservoir management by optimizing the economic life-cycle performance of the reservoir models [1-4]. The focus on such problems is related to the maximization of the recovery factor and economic parameters (e.g. net present value). Due to many non-unique possible solutions for a certain objective function, the optimization techniques are needed to achieve the improved one when initial oil rates have a considerable impact on the total oil production. There are many researches addressing different aspects of production scheduling. Van Essen et al. maximized short-term gains with a high discount rate by selecting the net present value (NPV) criteria as short-term gains [5]. According to the literature, NPV, which is a cumulative objective function, is maximized in life-cycle optimization techniques. In similar approaches used by Bailey et al. and Yasari et al., the goal was to minimize the variance of the NPV distribution and maximize the average NPV [6,7]. Siraj et al. used the explicit uncertainty handling in the model-based economic optimization to examine the balance between short-term and long-term gains [8]. In these life-cycle optimization techniques, NPV is maximized. Van Essen et al. proposed the robust optimization method including a model uncertainty in the optimization by considering an average NPV over an ensemble of geological model realizations [9]. They showed that their method led to a reduction of the variance of the optimized strategy and an increment of the expected value when applying to the different geological realization. Van Essen et al. used the adjoint formulation to attain robust optimization [5]; however when the adjoint approach is worked with commercial simulation, it needs to access to the simulation source code. Ikewun et al. has applied a decline curve for optimizing workflow. They exerted simulation models and the decline curve analysis (DCA) as a production optimization and forecasting tools for shale gas reservoirs [10]. Salam et al. introduced their approach to optimize production strategy which used the NPV; also, they considered the capital expenditure [11].

Proxy models and upscaling are two possible common solutions for fast objective function evaluation in the reservoir optimization. Proxy modeling is implemented in many field development and production optimization problems. The usage of a proxy function or a surrogate model is very effective to reduce the high computational cost of function evaluation for the numerical simulator. The neural network is used as an approximation optimization to reduce the number of simulation runs and represent the strongly non-linear behavior of a complex petroleum production system [12,13]. Onwunalu et al. combined an optimization algorithm with an enhanced statistical proxy led to speed up field development optimizations [14]. However, the neural network presents some practical difficulties where there are too many degrees of freedom or too many constraints, where the input space and the output space cannot be correlated at all, or where the learning costs of the neural network for difficult problems is high [15]. There are several approaches towards using proxy applications in the literature, including Neuro-Fuzzy [16], kriging [17,18], and statistical proxies [19].

Upscaling is interesting in the problems with high-resolution models. High-resolution geological models have been built to capture the heterogeneities of the reservoir. For typical history matching and prediction simulation studies, these models increase the computational cost and are time-consuming. Upscaling a reservoir model from the fine grid to a coarser grid has been performed for the simplification of reservoir models. By Usage of a quite accurate approach in which the cells of the fine model are merged together to form a single cell in the coarse model, an appropriate coarsening is achieved from a fine grid model that preserves a good estimate of the value of objective function (for more detailed information see King et al. [20]). Jessen et al. proposed a technique to simulate water flooding with coarse-scale dual-porosity [21]. In the early time, the performance of their approach could be acceptable in comparison with the fine model; however, at later times, due to the simplistic representation of flow and transport between active and passive porosities, it could not perform accurately. Chen et al. developed an upscaling model for near-well flow in heterogeneous reservoirs and improved the precision of standard upscaling methods [22].

Moreover, the need for fast objective function evaluation, selecting an appropriate automated optimization technique can provide a better production scenario. Ekkawong et al. used linear programming and decline curve analysis in a gas field with small compartmentalized reservoirs with several constraints [23]. Kritsadativud et al. used a gradient-based optimization algorithm with both linear and non-linear constraints in a single time-step [24]. The stochastic optimization algorithms are more effective for escaping from the local optima, due to continuing the search quite randomly in areas beyond attractive zones. There are also numbers of field applications of stochastic optimization techniques. The genetic algorithm (GA) has been applied to the optimization of well placement [14,25,26]. Morales et al. introduced a risk-constrained algorithm based on the GA to allow the user to input the risk factor desired and individual weights for each realization [27]. Their model provided different optimum well placement, which depended on the risk level wanted by the user to take. Guyaguler et al. used hybrid genetic algorithms based on the GA, polytope search, and Kriging Proxy to reduce the computational effort in the well place location optimization of injection wells under uncertainties [17]. A field development optimization procedure based on the GA and other optimization tools (neural networks and evolution strategies) has been proposed and applied to a number of reservoir models [11]. Other optimization algorithms, including simultaneous perturbation stochastic approximation, simulated annealing [28,29, 30], and particle swarm optimization have been applied to optimization problems [31, 32].

Managing water flooding is one of the most commonly used approaches toward improving oil recovery and reducing the costs, which requires to know about the amount of water injection and how to allocate it through injection wells. Indeed, the success of a water flooding project depends on the ability to sweep the remaining oil towards oil production wells. However, an improper design may result in increasing the costs associated with the water cycling and poor sweeping the remaining oil. Thiele and Batycky introduced well allocation factors (WAF) or injection efficiencies for each injector to optimize the amount of water injection and produced fluids between well pairs in a water flooding reservoir; then, the rate of injection was reallocated to improve the water flooding performance [33]. Also, Ghori et al. reported the application of this approach in the real field [34]. Alhuthali et al.

presented a streamline-based workflow to equalize the arrival time of the front of water flooding at all producers within selected sub-regions of a water flooding project [35]. Furthermore, Alhuthali et al. extended their study to optimize a water flooding under geological uncertainty [36]. Ambia proposed using the GA and the particle swarm optimization in water flooding problems to determine an optimum pattern design and production and injection strategy to maximize NPV of the project [31]. Van den Hoek et al. presented a new methodology combining fluid-flow and fracture-growth within the context of an existing standard reservoir simulator which was coupled with induced fractures via special connections to eliminate most of the numerical instabilities [37].

In the present work, the objective function that is NPV with a discount rate to consider the long-term and the short-term gains is optimized through the optimization of oil production rates and total water injection in a field sector in which the water injection is started from the beginning of the oil production. Initial guesses for oil production wells are related to the capacity of the production of each well. The adaptive simulated annealing (ASA) is combined with a polytope search to provide the optimization with the ability of escaping from the local minima. In the first iterations, using a coarse grid block model in ASA causes the time length of the life-cycle optimization strikingly to be reduced. In later iterations, the fine grid model is substituted to confirm the preciseness of the NPV value and fine-tuning of the optimization variables. In addition, the total water injection is allocated to each well by this workflow. The goal was to optimize the allocation of water injection well rates. The initial guesses for injection well rate allocation are determined by the injection efficiency or allocation factor of each well from the streamline simulation. Revision of all allocation water rates by considering a limited water cut led to control the water cut and the water production. The offered workflow is a new approach combined with two stages optimization (coarse grid-fine grid model) to allocate water injection rates and the usage of water allocation factor for the initial guess. In the next section, the approach is described in detail. Next, the case study results are presented to demonstrate the improvement in reducing the time length of the life-cycle optimization, when it keeps the precision of the final optimized solution.

EXPRIMENTAL PROCEDURES

Methodology

In this approach, the optimization of oil production rates of each well results in the optimization of total oil production. Furthermore, the reliability of the approach is improved by including practical constraints for the rates of each well. Later on, the optimized water injection rates allocation and revision of allocated water injection in each time step are led to an increase in the final objective function. The NPV is considered as the objective function in order to include both the long-term and the short-term gains. The objective function J is NPV for the cumulative oil and water production over a fixed time horizon which is introduced by Van Essen et al. [38] and can be expressed by the following mathematical formulation:

$$J=\sum_{K=1}^{K}\left[\frac{CWI^{K}+CWP^{K}-COP^{K}}{\left(1+b\right)^{\frac{t_k}{t_{ref}}}}\times\Delta t_k\right] \tag{1}$$

where, K shows the total number of time steps k, and Δt_k is the time interval of time step k in days. b is the discount rate for a certain reference time t_{ref}.

In the above objective function, the water injection cost is defined as:

$$CWI^{K} = \sum_{j=1}^{N_{inj}} r_{winj} \times q_{winj.k} \tag{2}$$

The produced water production cost is defined by:

$$CWP^{K} = \sum_{j=1}^{N_{prod}} r_{wp} \times q_{wp.k} \tag{3}$$

The produced oil production benefit is calculated by:

$$COP^{K} = \sum_{j=1}^{N_{prod}} r_{o} \times q_{o.k} \tag{4}$$

where, r_o , r_{wp}, and r_{winj} are the oil price, the water production cost, and the water injection cost in \$/m^3 respectively. $q_{winj.k}$, $q_{wp.k}$, and $q_{o.k}$ represent the total flow rate of injected water, produced water, and produced oil at time step *k* in m^3. N_{prod} and N_{inj} are the number of production and injection wells respectively. The optimization problem with the objective function defined in Equation 1 can be formulated as follows:

$$\max_{u_{1:K}} J(u_k), \tag{5}$$

Which is subject to:

$$g_{k+1}(u_k . x_k . x_{k+1}) = 0.\ k = 0.\ldots.K-1\, x_0 = \overline{x_0} \tag{6}$$

and

$$c_{k+1}(u_{k+1}.x_{k+1}) \leq 0\,. \tag{7}$$

where, u is the control vector (input vector), and x is the state vector (grid block pressures and saturations); g is a vector-valued function presenting the system equations, and x_0 stands for a vector of the initial conditions of the reservoir. A colon in a subscript indicates a range, e.g. $u_{1:K}$= {u_1, u_2,..., u_k}. The vector of inequality constraints g is related to the wells limitations.

The core optimization algorithm in this work is simulated annealing (SA) which has been introduced by Kirkpatrick [39]; in addition, it has been used as an optimization technique for the combinatorial optimization. SA is originated from the physical process of metallurgical annealing, when at first, a metal is at high temperature in a heating bath and is slowly cooled. Molecules in the hot metal are randomly dispersed. While the temperature is falling, the molecules are organized in a way, which is very near to the global minimum energy. The algorithm can escape the trap of local optimum by a metropolis algorithm using a random number generation method. The random search causes the algorithm to store variations which lead to decreasing the energy (objective function), and some variations increasing it [39]. If the new objective function is decreased, the set of optimization parameters will be accepted automatically. Otherwise, a Boltzmann probability function is called, and a random number is created. If the random number is less than the parameter set probability, it will be accepted as the next iteration:

$$P(accept) = \begin{cases} \Delta J < 0 & accept \\ \Delta J > 0 \rightarrow P = Exp\left(\dfrac{-\Delta J}{T}\right) \end{cases} \tag{8}$$

Boltzmann probability function depends on T being the temperature as a global time-varying parameter of the objective functions, i.e. J(uk_1) and J(uk_2). The SA algorithm can escape from a local minimum which is worse than the global one because the probability function P should be positive even when J(uk_2) is larger than J(uk_1). Adaptive simulated annealing (ASA) is an improved version of simulated annealing. In the first step of adaptive simulated annealing, i.e. the initial temperature, the initial solution should be entered, and the objective function should be initialized. Then, y^i, a random parameter introduced by Ingber [1] is defined in Equation 12 and helps create a random solution, α^{i}_{k+1} (in the problem, this is the initial rates for wells) which is defined in Equation 9. Also, α^{i}_{k} is the current solution in the dimension i generated at annealing-time *k* within the range, and $\boldsymbol{B}_i$ and $\boldsymbol{A}_i$ are the upper and lower bounds for α^{i}_{k}.

$$\alpha^i_{(k+1)} = \alpha^i_k + y^i (B_i - A_i) \quad (9)$$

$$y^i \in [-1,1] \quad (10)$$

y^i is generated from a u^i from the uniform distribution:

$$u^i \in U[0,1] \quad (11)$$

$$y^i = \mathrm{sgn}\left(u^i - \frac{1}{2}\right) T_i \left[\left(1 + \frac{1}{T_i}\right)^{|2u^i - 1|} - 1\right] \quad (12)$$

Finally, the value of objective function is calculated based on the new solution. The difference between two objective functions (delta) distinguishes whether the new solution is accepted or not. When the delta is equal or lower than zero, the new solution would be accepted, and the temperature based on a formulation proposed by Ingber [40] would be adjusted which is shown in Equation 13 and Equation 14, where T_{0i} is the initial temperature. Also, n_i and m_i can be considered free parameters to help tune ASA for specific problems. D is the dimension of the space problem. As it is represented in Figure 1, if the delta is greater than zero, the metropolis function is called. When the metropolis function is accepted, the new solution will be stored and the temperature will be adjusted by Equation 13. Otherwise, if the temperature is not reached the final temperature and rejected by the Boltzmann probability function, a new solution is generated in the algorithm. At the End, when the final temperature is reached, the algorithm will be terminated.

$$T_i(k) = T_{0i}\left(\exp\left(-c_i k^{\frac{1}{D}}\right)\right), \quad 0 < c < 1 \quad (13)$$

$$c_i = m_i \exp(-n_i / D) \quad (14)$$

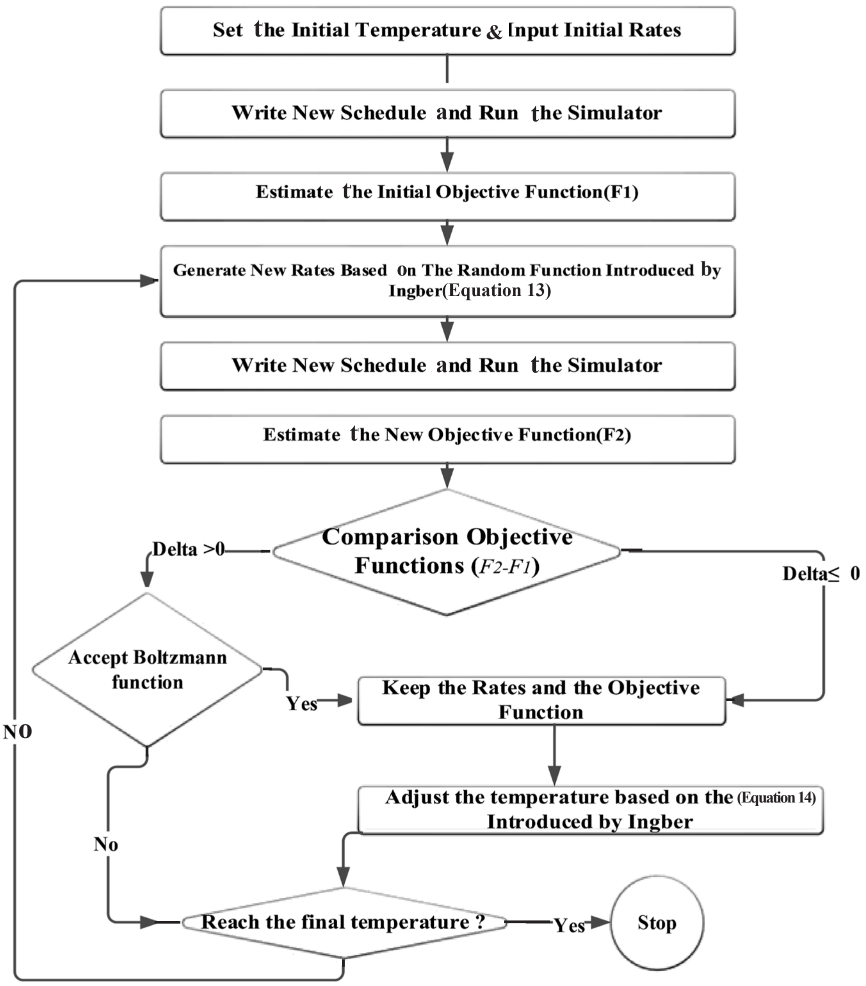

Figure 1: An adaptive simulated annealing flow diagram.

In the initial steps of adaptive simulated annealing (ASA), a coarse grid model is used which is created based on the horizon permeability map. This coarse grid model is used to reduce the length time needed to find the optimized solution. The optimization is performed in two sections; in the first section, the coarse grid block model is applied and does not have a substantial impact on the final solution because the solution varies in a large search space. In the second section, the fine grid block model is used to keep the preciseness of the final solution. Therefore, by dividing ASA in two sections of coarse and fine grid block models, the method can find an approximate optimized solution rapidly. By switching to fine grid section, the precise optimized solution can be guaranteed. Figure 2 shows the flowchart of ASA using fine grid and coarse grid models. The first guesses for the oil production rates in ASA come from their capacity of production, i.e. $NTGkhS_o$ where NTG, k, h, and S_o are net to gross, permeability, height, and oil saturation respectively. This makes a reliable guess for all rates of production wells and helps accelerate the optimization by improving the next guess. The initial oil rates and the total water injection are the input and the objective function calculated through the amount of oil and water production. Until the temperature is got to a specified temperature, the coarse grid block model is applied. In addition, a polytope search, a hill-climbing algorithm, enhances the speed of the method by finding the best solution between the previous iterations and picking the best one for the next guess in the ASA. The polytope algorithm introduced by Nelder and Mead tries to find the direction that increases the value of the objective function. In the next step, the fine grid block model is used when the temperature does not reach the final temperature, i.e. the stopping criteria.

To simulate the water flooding process, the coupled system of non-linear equations system for oil and water material balance for each simulation cell should be solved in ECLIPSE.

In the presented method, water injection rate allocation is performed after the optimized total amount of water injection has been determined. This allocation is done by using the same workflow for finding the optimized oil production rates. This means a two-stage ASA (coarse and fine grid block models) is used to be coupled with a polytope search to speed up the process. The speed of the usage of the coarse grid block model and the accuracy of the solution in the section of fine grid block model help optimize the allocation of water injection by an efficient workflow. For finding a trustworthy initial allocated injection water rate, water well allocation factor is an acceptable clue to assign an appropriate water injection rate to each well. Well allocation factor is the ratio of injected water to the oil produced at offset wells, which allows us to calculate the efficiency of injection wells calculated by the streamline based on flow simulation. Injection efficiency introduced by Thiele and Batycky [33] is defined as follows:

$$I_{eff} = \frac{\text{off}-\text{set oil production}\left[\text{rb}/\text{day}\right]}{\text{water injection}\left[\text{rb}/\text{day}\right]} \qquad (15)$$

At optimized oil production rate, water injection rates are allocated. The well allocation factor comes from streamline simulation in each time step, and then the average of the total time steps for each injection well is calculated. By the allocation of the water injection rate to each well, the more remaining oil is swept towards oil production wells. The improved sweep efficiency provides a higher objective function and satisfies the economic consideration such as the reduction of the total amount of water production and the total oil production increment. A revision of the allocation rates during oil production and water injection results in better total water production controls, and the breakthrough time by specifying the economical operation limits of the wells such as water cut. If a well violates the limitation value such as specified water cut, the worst offending connection, which has the highest water cut in the well, will be closed. Even the entire well will be shut down in a case of very high water cut. This remedy has a considerable effect on the reduction of the total water production and the water cut; moreover, this remedy postpones the breakthrough of water injected front. Because of decreasing the total water production, the cost of water production is declined significantly. Therefore, it increases the value of the objective function.

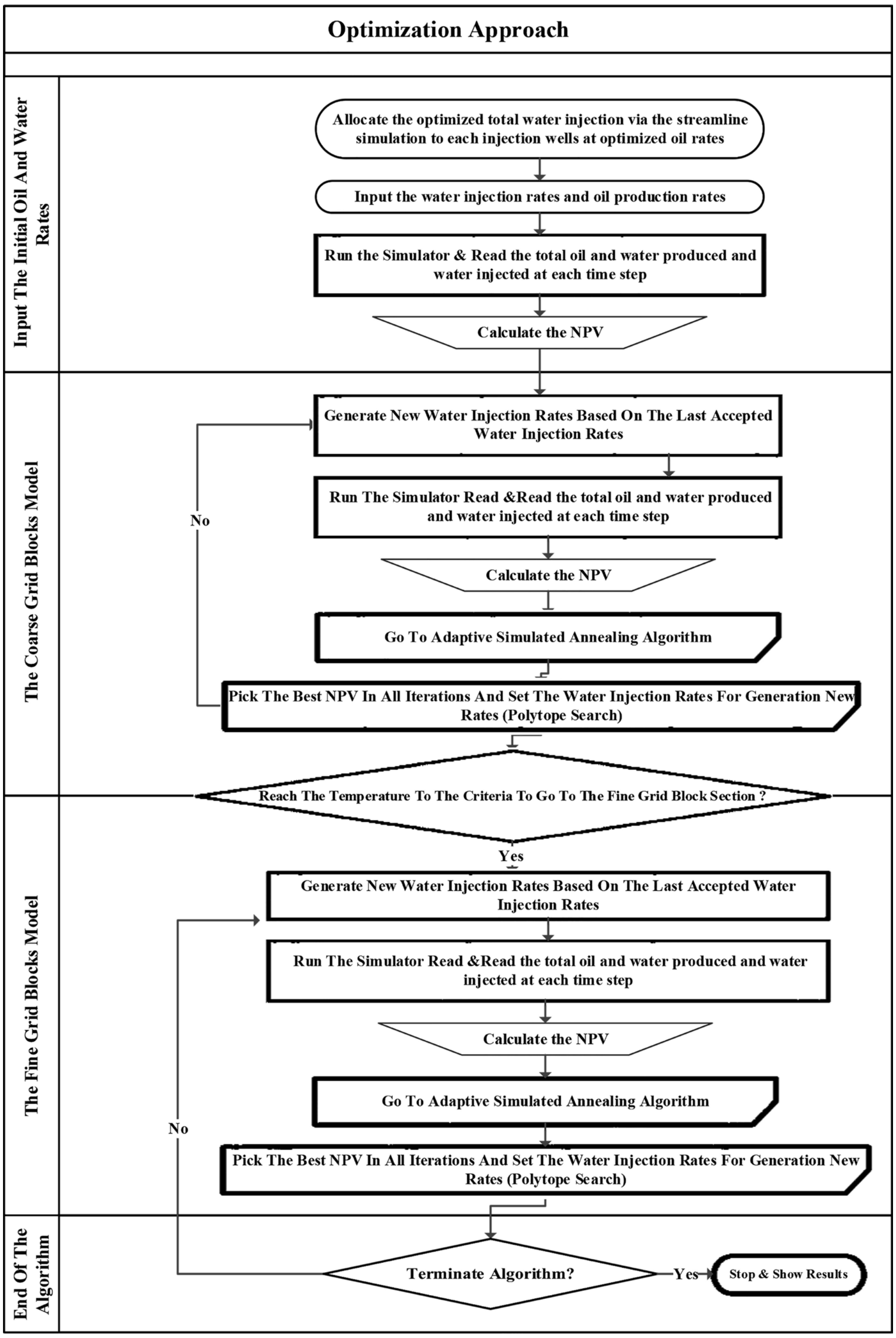

Figure 2: Workflow of the Optimization Algorithm.

RESULTS AND DISCUSSION

The optimization procedure was applied to a sector of a real three-dimensional oil reservoir model with two phases (water and oil) in Libya. The mentioned field sector named Mudarko was given to the authors for this research work. The reservoir model consists of 47310 (83×114×5) grid blocks, 14 injection wells, and 33 production wells. The control mode of production was on the liquid production rate. The life cycle of the reservoir covered a period of 24820 days. The initial and bubble point pressure were 641.5 and 267.93 psi respectively. The distribution of the porosity and the permeability is shown in Figure 3.

The reservoir porosity is ranging from zero to 0.15. According to the porosity map, the lower part of the figure exhibits very low porosity (very low quality rock) which shows a barrier-like behavior. This makes the average porosity in the reservoir to be 0.056.

It should be noted that the permeability in the all directions is the same, and it changes from 4.2 to 1028 mD. All remaining geological and fluid properties used in the model are presented in Table 1 and Table 2.

Table 1: Geological and fluid properties of the model

Property	Value	Units
ϕ	0.05759	-
ρ_o(at 14.7 psi)	847.376534	kg/m^3
ρ_w (at 14.7 psi)	1117.316	kg/m^3
c_o (at $_{Pint}$)	1.459E-05	1/psi
c_w (at $_{Pint}$)	4.579e-006	1/psi
μ_o (at $_{Pint}$)	0.3289	Pa.s
μ_w (at $_{Pint}$)	0.5	Pa.s
Temperature	87	°C

Table 2: Statistical information of simulation grid blocks dimensions

	Min (m)	Max (m)	Delta (m)	Mean (m)	Std. dev.	Variance
DX	9.74	17.12	7.37	13.14	1.93	3.72
DY	501.75	501.81	0.06	501.75	0.02	0
DZ	498.75	498.88	0.13	498.8	0.06	0

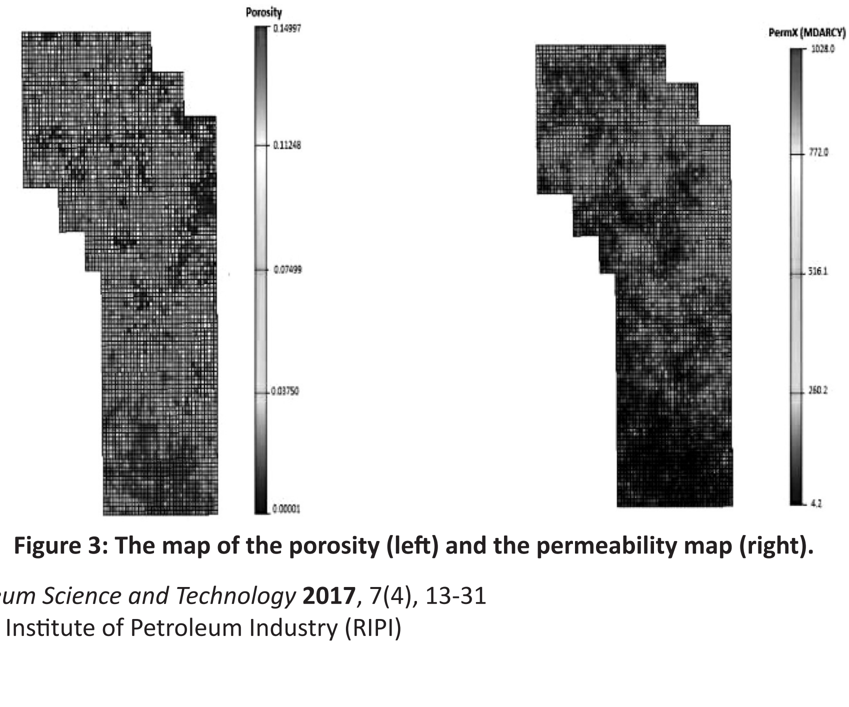

Figure 3: The map of the porosity (left) and the permeability map (right).

The coarse grid model contains 1150 grid blocks, so the number of grid blocks is significantly decreased. The upscaling procedure is performed in a very careful procedure based on the visual contrast in the permeability as can be seen from Figure 4. This produces a suitable coarse scale model with a production behavior such as the field pressure decline and the oil production rate close to fine scale one as shown in Figure 5. However, everything is not exactly the same, especially if it is investigated well by well. The time elapsed for the fine grid model and coarse grid one are 413.32 and 54.94 seconds respectively. A substantial speed-up is achieved by this short run time.

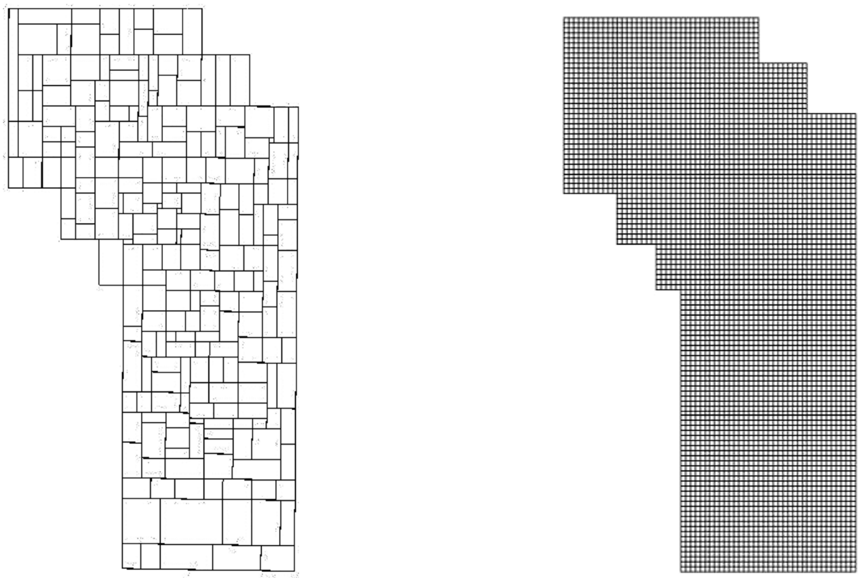

Figure 4: The coarse grid model (left) and the fine grid model (right).

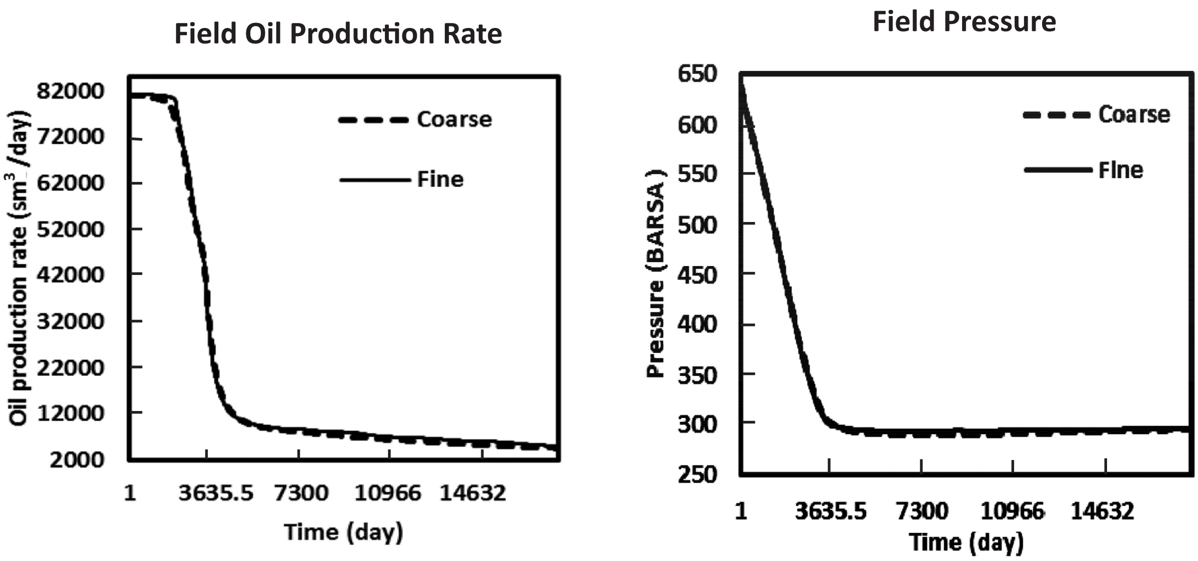

Figure 5: Field oil production rate versus time for both model coarse and fine models (left), and field pressure versus time for both model coarse and fine models (right).

Through implementing the optimization approach, the optimized total oil production can be found. NPV, the objective function defined in Equation 1, is codded in C# programming language and coupled with ECLIPSE for simulation runs where r_o = 128 \$/m^3 (20.33 \$/bbl), r_w=19 \$/m^3 (3.02 \$/bbl), and r_{inj}=6 \$/m^3(0.95 \$/bbl). The minimum initial oil rate production for all production wells is defined 500 m^3/day, and the maximum water injection rate for all injection wells is defined to be 10000 m^3/day as practical constraints in the optimization method. The optimized scenario was selected among 567 scenarios created in the ASA algorithm. In the context of optimization, there are two words that those are used sometimes instead of each other: optimized solution and optimal solution. However, some authors distinguish between the two words. The optimal solution is the global maximum; however, the optimized solution is a solution improved from the starting point and closer to the global maximum. The algorithm, which has been used for optimization, is a stochastic optimization procedure. Such procedure can investigate the variables space with several different directions due to Metropolis algorithm. The outcome of the stochastic procedure is different for two different runs. The optimization repetition also helped us to select among the best results.

As the result shows in Figure 6, although the initial oil production rate of optimized scenario was substantially lower than the first guess for the oil production rate, the total field oil production was increased from 385.983 *Msm*^{3} (the initial guess) to 440.656 *Msm*^{3}, i.e. 14.16% increment. Due to increasing water injection from 18100 m^3/day to 25073 m^3/day in the optimized solution, more oil was swept to the oil production wells. Therefore, another scenario was performed with the optimized total water injection rate and the initial oil production rates, which is simply called initial scenario with an optimized injection. This means that the oil production rates and total water injection rate are subject to optimization. The result revealed that the total optimized oil production is still 2.20% better than this scenario (see Figure 6). In addition, a recovery factor comparison is displayed in Figure 7; the recovery factor for the optimized scenario is 32.24%, which is higher than the recovery factors of the initial scenario (28.22%) and the initial scenario with the optimized injection (31.51%).

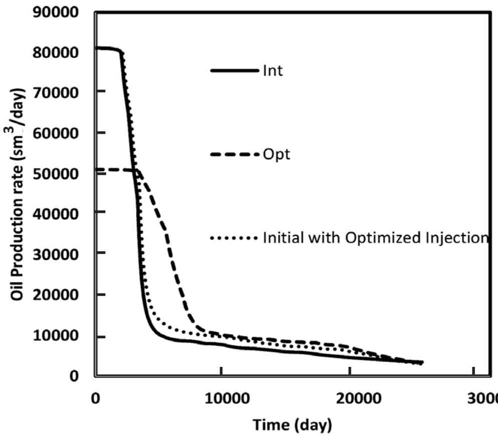

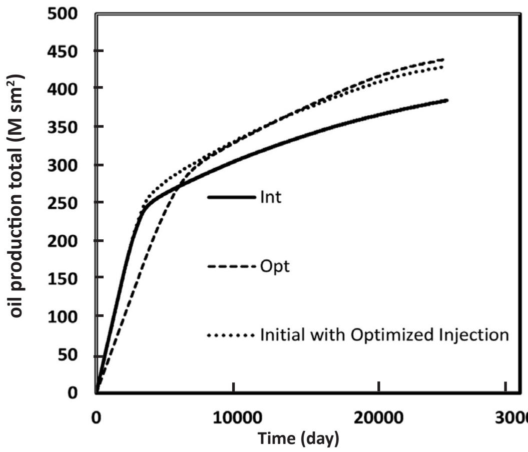

Figure 6: Field oil production rate, comparison between the initial scenario and Initial with optimized injection (dotted line) (left); total field oil production comparison between the initial scenario (solid line) and Initial with optimized injection (dotted line) (right).

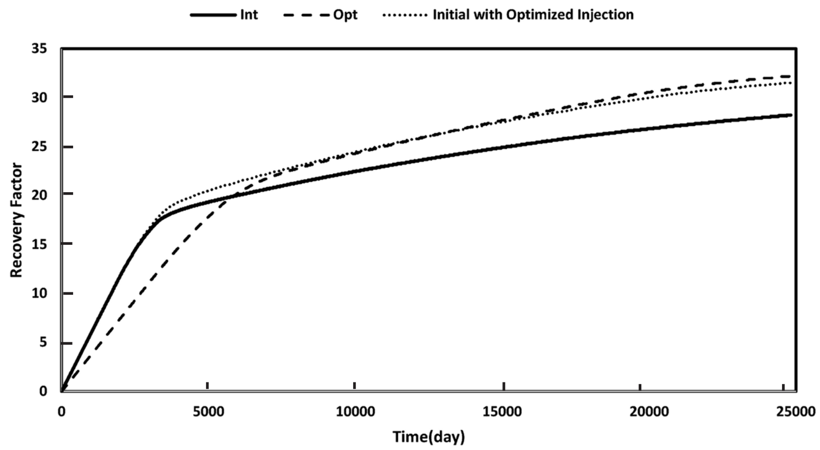

Figure 7: Recovery factor comparison between the initial scenario (solid line) and the initial scenario with optimized injection (dotted line).

In Figure 8 to Figure 9, oil production rates and the total oil production for two wells in the optimized scenario, initial scenario, and initial scenario with optimized injection are presented. There are cases for which, the optimized total oil production is higher than other scenarios; however, the initial oil rate of the optimized wells is lower than that of others. Furthermore, it should be noted that if the plots, one by one, for all wells are check, not all the total oil production of wells in the optimized scenario have a better result than the first scenario. Indeed, the general effect of all of the wells in the optimized scenario has a higher outcome. Figure 10 shows the objective function in each iteration. The polytope search helps the objective function to have an ascending profile.

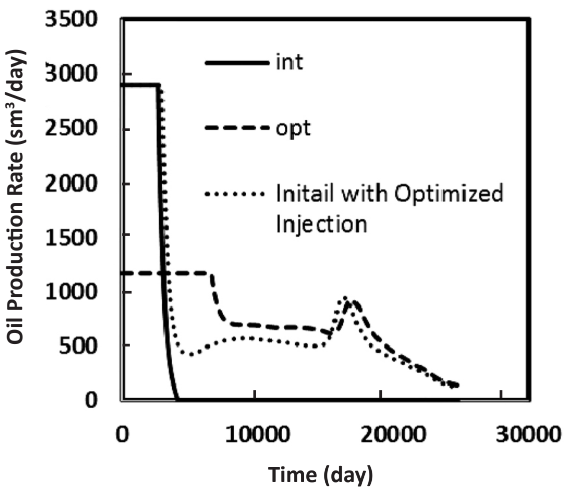

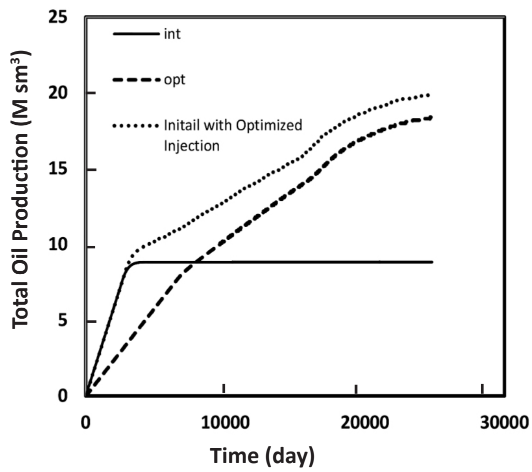

Figure 8: Oil production rates comparison in well M_P12-3 (left); the total oil production comparison in well M_ P12-3, among optimum scenario, initial scenario, and initial scenario with optimized water injection (optimized the total water injection rate and the initial oil production rates) (right).

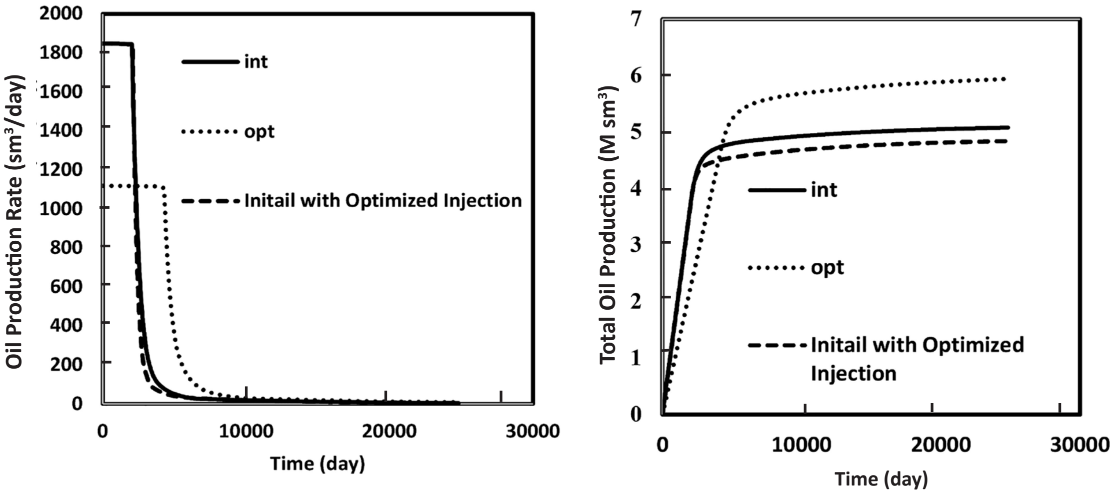

Figure 9: Oil production rates comparison in well M_P13-4 (left); the total oil production comparison in well M_P13-4, among optimum scenario, initial scenario, and initial scenario with optimized water injection (optimized the total water injection rate and the initial oil production rates) (right).

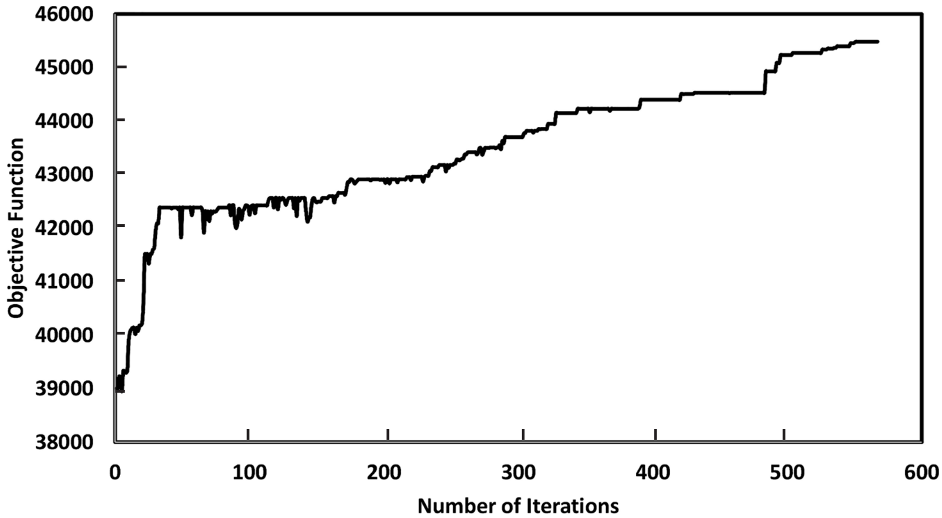

Figure 10: Objective function versus the number of iterations.

In the next step, the total water injection, which was calculated from the optimized scenario, is allocated to each injection well by a new workflow. For simplicity, this optimization of water injected allocation (water injection rate allocation in the injection well) is called the allocation scenario. For finding the optimized water allocation scenario, 567 scenarios are created in the ASA algorithm by being codded in C# programming language and being coupled with ECLIPSE for simulation runs at the same oil production rates calculated from the optimized oil production scenario. The mentioned optimization workflow was used to allocate water injection at the optimized oil production rates, which were calculated from previous optimization. For the first guess to allocate water injection, the water allocation factor calculated by streamline simulation was used in order to allocate total optimized water injection. There is not too much difference between the initial water allocation rates which come from streamline simulation and the final result for water injection wells which come from the presented method. Hence, the first allocation factors are an acceptable optimized water allocation. Moreover, the revision of water allocation rates considered some economic constraints for water cut and minimum oil production rate at the optimized oil production scenario. The allocation of water injection can have a significant effect on the improvement of the water flooding efficiency. In fact, the optimized total water injection rate should be distributed over water injection wells in a way that most of the remaining oil can be produced. As we can see in Figure 11, by making a comparison between the optimized oil production scenario, which is achieved from the previous optimization of oil production rates, and total water injection (the optimized oil scenario), the optimization of the allocation of water injection rates scenario (allocation scenario) and the total oil production are represented as 450.164 Msm^3 and 440.565 Msm^3 respectively. In addition, a recovery factor comparison is presented in Figure 12; moreover, the recovery factor is improved from 32.24% (the optimized oil scenario) to 32.91% (the allocation scenario). Although the total oil production does not have a remarkable improvement, the total water production in the allocation and revision scenario is strikingly decreased (Figure 13). The total water produced in the optimized oil scenario and the allocation scenario was 201.117 Msm^3 and 132.427 Msm^3 respectively; in other words, the total water produced was decreased by about 35%. However, the total water injection in the allocation scenario was increased by 4%. Water injection rates allocation helped decrease the water produced; therefore, the cost of water produced was decreased, and the total benefit was improved. Water cut shown in the Figure 14 also demonstrates that during the production the water cut in the allocation scenario is lower than the optimized oil. Considering all of the mentioned information such as the increment in the total oil production, the reduction in the total water production, and the improvement in controlling water cut during the life cycle of the reservoir leads to the enhancement of the objective function in the revision of water rate allocation scenario. This means gaining more profit and a reduction in the costs of water production and injection as shown in Figure 15. The optimized objective function for the allocation scenario was 48800, while the optimized objective function of the optimized oil scenario was 45400.

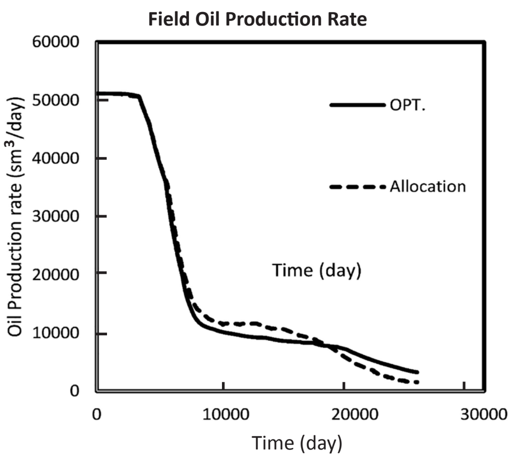

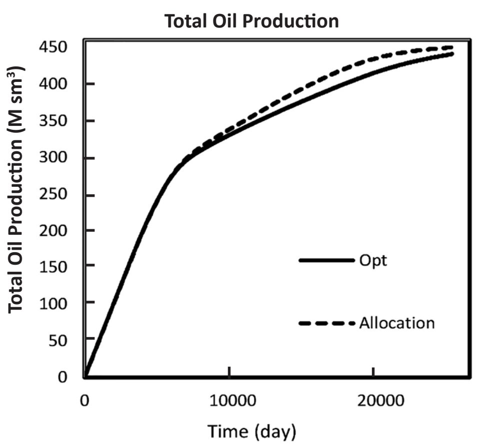

Figure 11: Field oil production rates comparison between the optimized oil scenario and the allocation scenario (left); total oil production comparison between the optimized oil scenario and the allocation scenario (right).

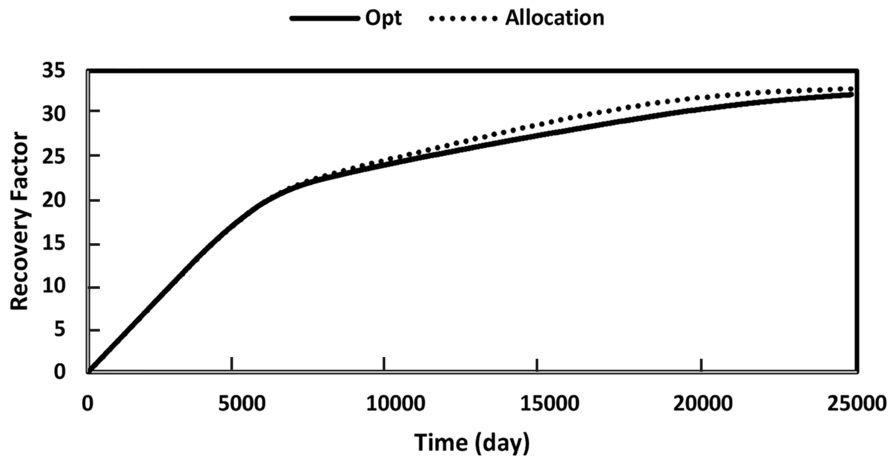

Figure 12: Recovery factor between the optimized oil scenario and allocation scenario.

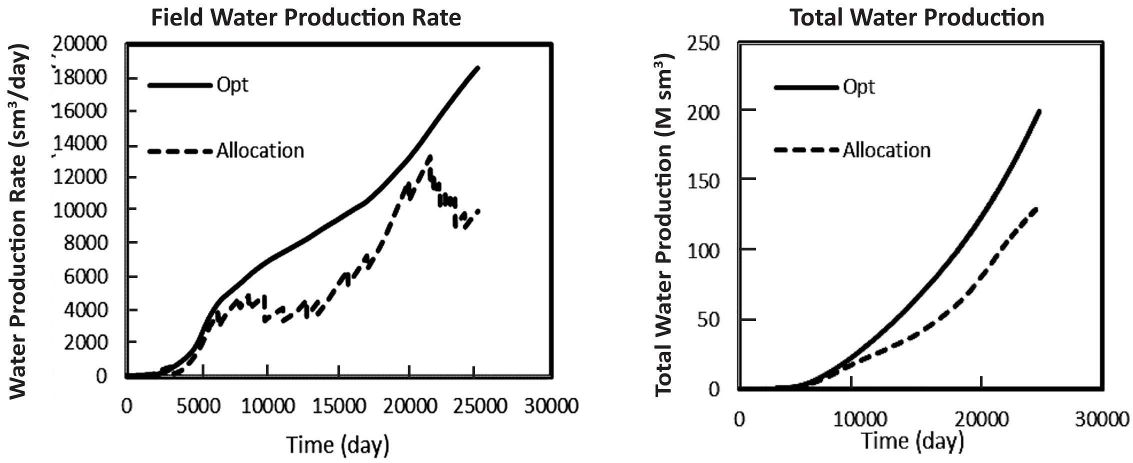

Figure 13: Field water production rates comparison between the optimized oil scenario and the allocation scenario (left); total water production comparison between the optimized oil scenario and the allocation scenario (right).

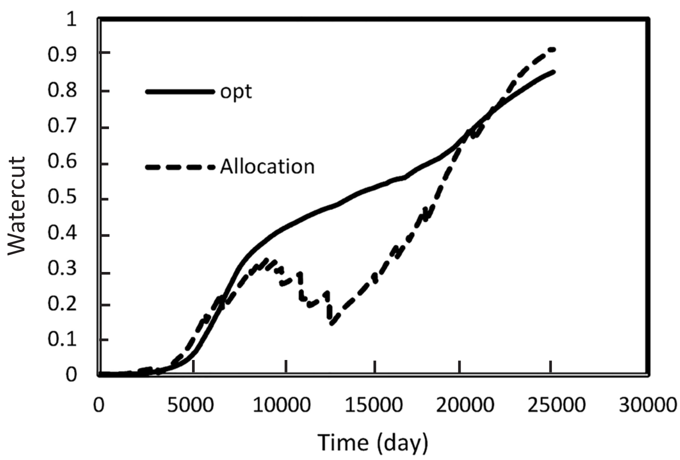

Figure 14: Water cut comparison between the optimized oil scenario and the allocation scenario.

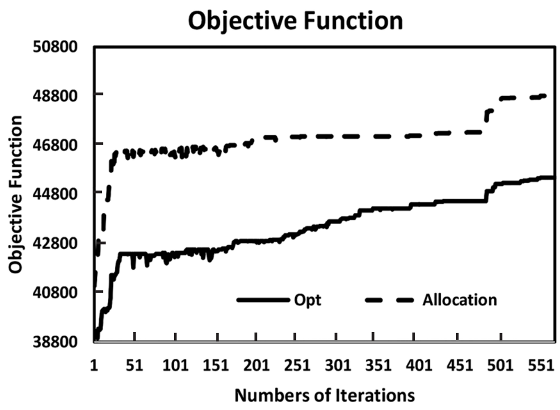

Figure 15: objective functions comparison between the optimized oil scenario and the allocation scenario.

The uncertainty in NPV comes from both the modeling process of water flooding and varying economic conditions, which include economic variables such as the interest rate, oil price etc. Including these uncertainties can be a step further in the future research to improve the optimization objective function definition, and to create a more reliable solution.

CONCLUSIONS

In this work, an effective scheme was offered to use a two-level adaptive simulated annealing technique for the optimization of initial oil production rates and total water injection in a reservoir undergoing water flooding and the allocation of water injection rates to each injection well. This method noticeably causes the run time of the optimization process to be decreased relative to the direct optimization. The objective function is based on NPV to consider the long-term and short-term gains. Based on the numerical simulation, it is concluded that:

• The optimization of oil well rates is an important issue in the total oil recovery. Consequently, the initial oil rate selection for wells should be accurate. To escape from the local minima during multi-variables optimization workflow, the usage of stochastic optimization algorithms such as ASA including Metropolis mechanism aids the optimization procedure.

• Using the coarse grid model for the early temperature cooling in ASA algorithm provides the optimization approach with reducing the run time of the optimization. The coarsening of the grid blocks based on the permeability map is performed, and reducing the number of grid blocks has a considerable effect on the performance of the proposed optimization for the first stage of optimization. For the final steps, the fine grid blocks model was used to keep the accuracy and reliability of the solution. The comparable trends of reservoir behavior such as field pressure decline and oil production rates in both of the fine and coarse grid models are necessary factors to generate a reliable coarse grid model.

• The optimized total water injection can be allocated through the proposed workflow for each injection well. The allocated water injection rates not only increase the total oil production, but also decrease the total water production.

• The revision of allocated water helps the method to consider some economic constraints, e.g. for water cut. This revision leads to better control on the water cut.

• The water allocation factors calculated from streamline simulation provide the acceptable initial water injection rates for the allocation of total water injection.

NOMENCLATURES

Δt_k	: time interval of time step k (y)
ASA	: Adaptive simulated annealing
b	: discount rate
c	: compression (1/psi)

GA	: Genetic algorithm
J	: objective function
k	: time step counter
NPV	: Net present value ($)
NTG	: net to gross
o	: oil
p	: pressure (bar)
q	: rate production/injection
r	: revenues/costs
S	: saturation
SA	: Simulated annealing Subscripts
t_k	: time at time step k (date)
t_{ref}	: reference time (date)
u	: input vector
w	: water
winj	: Injected water
wp	: produced water
x	: state vector
x_0	initial conditions
μ	: viscosity (cp)
ρ	: density (kg/m^3)
φ	: porosity

REFERENCES

1. Asheim H., “Maximization of Water Sweep Efficiency by Controlling Production and Injection Rates,” *European Petroleum Conference*, London, United Kingdom, **1988**.
2. Sudaryanto B. and Yortsos Y. C., “Optimization of Fluid front Dynamics in Porous Media Using Rate Control. I. Equal Mobility Fluids,” *Physics of Fluids* (1994-present), **2000**, *12*, 1656-1670.
3. Brouwe D. and Jansen J., “Dynamic Optimization of Water Flooding with Smart Wells Using Optimal Control Theory,” *European Petroleum Conference*, Aberdeen, United Kingdom, **2002**.
4. Sarma P., Aziz K., and Durlofsky L. J., “Implementation of Adjoint Solution for Optimal Control of Smart Wells,” *SPE Reservoir Simulation Symposium*, The Woodlands, Texas, **2005**.
5. Van Essen G., Van den Hof P., and Jansen J. D., “Hierarchical Long-term and Short-term Production Optimization,” *SPE Journal*, **2011**, *16*, 191-199.
6. Bailey W. J. and Couet B., “Field Optimization Tool for Maximizing Asset Value,” *SPE Reservoir Evaluation & Engineering*, **2005**, *8*, 7-21.
7. Yasari E., Pishvaie M. R., Khorasheh F., Salahshoor K., and et al., “Application of Multi-criterion Robust Optimization in Water-flooding of Oil Reservoir,” *Journal of Petroleum Science and Engineering*, **2013**, *109*, 1-11.
8. Siraj M. M., Van den HofP. M., and Jansen J. D., “Model and Economic Uncertainties in Balancing Short-Term and Long-Term Objectives in Water-Flooding Optimization,” *SPE Reservoir Simulation Symposium*, Houston, Texas, **2015**.
9. van Essen G., Zandvliet M., Van den Hof P., Bosgra O., and et al., “Robust Water Flooding Optimization of Multiple Geological Scenarios,” *SPE Journal*, **2009**, *14*, 202-210.
10. Ikewun P. O. and Ahmadi M., “Production Optimization and Forecasting of Shale Gas Wells Using Simulation Models and Decline Curve Analysis,” *SPE Western Regional Meeting*, Bakersfield, California, USA, **2012**.
11. Salam D. D., Gunardi I., and Yasutra A., “Production Optimization Strategy Using Hybrid Genetic Algorithm,” in *Abu Dhabi International Petroleum Exhibition and Conference*, Abu Dhabi, **2015**.
12. Yeten B., “Optimum Deployment of Nonconventional Wells,” Stanford University, **2003**.
13. Zangl G., Graf T., and Al-Kinani A., “Proxy Modeling in Production Optimization,” *SPE*

Europec/EAGE Annual Conference and Exhibition, **2006**.
14. Onwunalu J. E., Litvak M. L. , Durlofsky L. J., and Aziz K., "Application of Statistical Proxies to Speed up Field Development Optimization Procedures," *Abu Dhabi International Petroleum Exhibition and Conference*, Abu Dhabi, **2008**.
15. Carpenter W. C. and Barthelemy J. F., "A Comparison of Polynomial Approximations and Artificial Neural Nets as Response Surfaces," *Structural Optimization*, **1993**, *5*, 166-174.
16. Zarei F., Daliri A., and Alizadeh N., "The Use of Neuro-fuzzy Proxy in Well Placement Optimization," *Intelligent Energy Conference and Exhibition*, Amsterdam, The Netherlands, **2008**.
17. Guyaguler B. and Horne R. N., "Uncertainty Assessment of Well Placement Optimization," *SPE Annual Technical Conference and Exhibition*, New Orleans, Louisiana, **2001**.
18. Schuetter J., Mishra S., Zhong M., and LaFollette R., "Data Analytics for Production Optimization in Unconventional Reservoirs," *Unconventional Resources Technology Conference*, San Antonio, Texas, USA, **2015**.
19. Artus V., Durlofsky L. J., Onwunalu J., and Aziz K., "Optimization of Nonconventional Wells under Uncertainty Using Statistical Proxies," *Computational Geosciences*, **2006**, *10*, 389-404.
20. King M. J., Burn K. S., Wang P., Muralidharan V., et al., "Optimal Coarsening of 3D Reservoir Models for Flow Simulation," *SPE Annual Technical Conference and Exhibition*, Dallas, Texas, **2005**.
21. Jessen K. and Evazi Yadecuri M., "Simulation of Water Flooding with Coarse-scale Dual-porosity Representation of Highly Heterogeneous Reservoirs," *SPE Western Regional & AAPG Pacific Section Meeting 2013 Joint Technical Conference*, Monterey, California, USA, **2013**.
22. Chen Y., Bernath A., Rai H., and Muron P., "Development and Application of Upscaling Techniques for Modeling Near-well Flow in Heterogeneous Reservoirs," *SPE Annual Technical Conference and Exhibition*, Orleans, Louisiana, **2009**.
23. Ekkawong P., Kritsadativud P., Lerlertpakdee P., and Amornprabharwat A., "Innovative and Automated Workflow for Fast Production Optimization and Forecast in Gulf of Thailand Gas Fields Using Linear Programing Optimization," *SPE Digital Energy Conference and Exhibition*, The Woodlands, Texas, USA, **2015**.
24. Kritsadativud P., Jafarpour B., and Ekkawong P., "Fast Production Optimization with Decline Curve Analysis Under Facility Constraints: A Field Case Study," *SPE Western Regional Meeting*, Garden Grove, California, USA, **2015**.
25. Emerick A. A., Silva E., Messer B., Almeida L. F., et al., "Well Placement Optimization Using a Genetic Algorithm with Nonlinear Constraints," *SPE reservoir simulation symposium*, The Woodlands, Texas, **2009**.
26. Kazakov K. V. and Bravichev K. A., "Automated Way to Search for the Optimum Irregular Well Placement Using a Genetic Algorithm (Russian)," *SPE Russian Petroleum Technology Conference and Exhibition*, Russia, **2016**.
27. Morales A. N. , Nasrabadi H., and Zhu D., "A New Modified Genetic Algorithm for Well Placement Optimization under Geological Uncertainties," *SPE EUROPEC/EAGE Annual Conference and Exhibition*, Vienna, Austria, **2011**.
28. Castaño K. P. and Ojeda G., "Optimizing Thin-

layer Mapping through Spectral Inversion: Performance of Genetic Algorithms and Simulated Annealing," *2010 SEG Annual Meeting*, Denver, Colorado, **2010**.

29. Khan H., Saputelli L. A., Ranjan P., Carvajal G. A., et al., "Multi-Objectives Constrained Water flood Optimization in Tight Carbonates," *SPE Reservoir Characterization and Simulation Conference and Exhibition*, Abu Dhabi, UAE, **2013**.
30. Yang D., Zhang Q., and Gu Y., "Integrated Optimization and Control of the Production-injection Operation Systems for Hydrocarbon Reservoirs," *Journal of petroleum science and Engineering*, **2003**, *37*, 69-81.
31. Ambia F., "A Robust Optimization Tool Based on Stochastic Optimization Methods for Water Flooding Project," *SPE Annual Technical Conference and Exhibition*, San Antonio, Texas, USA, **2012**.
32. Lagos S. R., Sabbione J. I., and Velis D. R., "Very Fast Simulated Annealing and Particle Swarm Optimization for Microseismic Event Location," *2014 SEG Annual Meeting*, Denver, Colorado, USA, **2014**.
33. Thiele M. R. and Batycky R., "Water Injection Optimization Using a Streamline-based Workflow," *SPE Annual Technical Conference and Exhibition*, Denver, Colorado, **2003**.
34. Ghori S. G., Jilani S. Z., Alhuthali A., Krinis D., et al., "Improving Injector Efficiencies Using Streamline Simulation: A Case Study in a Giant Middle East Field," *SPE Middle East Oil and Gas Show and Conference*, Manama, Bahrain, **2007**.
35. Alhuthali A., Oyerinde A., and Datta-Gupta A., "Optimal Water Flood Management Using Rate Control," *SPE Annual Technical Conference and Exhibition*, San Antonio, Texas, USA, **2006**.
36. Alhuthali A. H. H., Datta-Gupta A., Yuen B. B. W., et al, "Optimal Rate Control under Geologic Uncertainty," *SPE Symposium on Improved Oil Recovery*, Oklahoma, USA, **2008**.
37. Van Den Hoek P. J., Al-Masfry R. A., Zwarts D., Jansen J. D., et al., "Waterflooding Under Dynamic Induced Fractures: Reservoir Management and Optimization of Fractured Water Floods," *SPE Symposium on Improved Oil Recovery*, Tulsa, Oklahoma, USA, **2008**.
38. Van Essen G., Jansen J. D., and Van den Hof P., "Hierarchical Long Term and Short Term Production Optimization," *Society of Petroleum Engineers*, New Orleans, Louisiana, **2009**.
39. Kirkpatrick S., "Optimization by Simulated Annealing: Quantitative Studies," *Journal of Statistical Physics*, **1984**, *34*, 975-986.
40. Ingber L., "Adaptive Simulated Annealing (ASA): Lessons learned," *Control and Cybernetics*, **1996**, *25*, 33-54.